

A refined exponential shear deformation theory for free vibration of FGM beam with porosities

Lazreg Hadji^{*1,2}, T. Hassaine Daouadji^{1,2} and E. Adda Bedia²

¹ Université Ibn Khaldoun, BP 78 Zaaroura, 14000 Tiaret, Algérie

² Laboratoire des Matériaux & Hydrologie, Université de Sidi Bel Abbès, 22000 Sidi Bel Abbès, Algérie

(Received March 10, 2015, Revised May 01, 2015, Accepted May 08, 2015)

Abstract. In this paper, a refined exponential shear deformation theory for free vibration analysis of functionally graded beam with considering porosities that may possibly occur inside the functionally graded materials (FGMs) during their fabrication. For this purpose, a new displacement field based on refined shear deformation theory is implemented. The theory accounts for parabolic distribution of the transverse shear strains and satisfies the zero traction boundary conditions on the surfaces of the beam without using shear correction factors. Based on the present refined shear deformation beam theory, the equations of motion are derived from Hamilton's principle. The rule of mixture is modified to describe and approximate material properties of the FG beams with porosity phases. The accuracy of the present solutions is verified by comparing the obtained results with the existing solutions. Illustrative examples are given also to show the effects of varying gradients, porosity volume fraction, aspect ratios, and thickness to length ratios on the free vibration of the FG beams.

Keywords: functionally graded beam; shear deformation theory; porosity; vibration

1. Introduction

Functionally graded materials (FGMs) have many advantages for use in engineering structural components. Unlike fiber-matrix laminated composites, FGMs do not have problems of de-bonding and delaminating that result from large inter-laminar stresses. The concept of FGMs was initially introduced in the mid-1980s by Japanese scientists. FGMs are microscopically inhomogeneous and spatial composite materials which are usually composed of two different materials such as a pair of ceramic-metal or ceramic-polymer. The composition of the material changes gradually throughout the thickness direction. As a result, mechanical properties are assumed to vary continuously and smoothly from the top surface to the bottom. Due to good characteristics of ceramics in heat and corrosive resistances combined with the toughness of metals or high elastic of polymers, the combination of ceramics and metals or polymers can lead to excellent materials. The FGMs are widely used in mechanical, aerospace, nuclear, and civil engineering. Consequently, studies devoted to understand the static and dynamic behaviors of FGM beams, plates have being paid more and more attentions in recent years.

*Corresponding author, Ph.D., E-mail: had_laz@yahoo.fr

Zhong and Yu provided an analytical solution for cantilever beams subjected to various types of mechanical loadings using the Airy stress function. Bending analysis of FG beams based on higher order shear deformation under ambient temperature was investigated by Kadoli *et al.* (2008). Li (2008) investigated static bending and transverse vibration of FGM Timoshenko beams, in which by introducing a new function, the governing equations for bending and vibration of FGM beams were decoupled and the deflection, rotational angle and the resultant force and moment were expressed only in the terms of this new function.

Sallai *et al.* (2009) investigated the static responses of a sigmoid FG thick beam by using different beam theories. Benatta *et al.* (2009) presented a mathematical solution for bending of short hybrid composite beams with variable fibers spacing. Şimşek (2010a) studied the free vibration analysis of an FG beam using different higher order beam theories. In a recent study, Şimşek (2010b) has studied the dynamic deflections and the stresses of an FG simply-supported beam subjected to a moving mass by using Euler–Bernoulli, Timoshenko and the parabolic shear deformation beam theory. Giunta *et al.* (2011) used the Hierarchical theories for the free vibration analysis of functionally graded beams. Thai and Vo (2012) investigated the Bending and free vibration of functionally graded beams using various higher-order shear deformation beam theories. Hadji *et al.* (2014) studied the bending and vibration responses of FG beams via a higher shear deformation beam theory. Bourada *et al.* (2012) proposed a new four variable refined plate theory for thermal buckling analysis of functionally graded sandwich plates. Nedri *et al.* (2014) studied the free vibration analysis of laminated composite plates resting on elastic foundations by using a refined hyperbolic shear deformation theory. Klouche Djedid *et al.* (2014) used a n-order four variable refined theory for bending and free vibration of functionally graded plates. Ait Yahia *et al.* (2015) investigated the wave propagation in functionally graded plates with properties using various. Merazi *et al.* (2015) proposed a new hyperbolic shear deformation plate theory for static analysis of FGM plate based on neutral surface position.

However, in FGM fabrication, micro voids or porosities can occur within the materials during the process of sintering. This is because of the large difference in solidification temperatures between material constituents (Zhu *et al.* 2001). Wattanasakulpong *et al.* (2012) also gave the discussion on porosities happening inside FGM samples fabricated by a multi-step sequential infiltration technique. Therefore, it is important to take in to account the porosity effect when designing FGM structures subjected to dynamic loadings.

In this paper, a variationally consistent shear deformation theory is developed using a new displacement field for thick FG beams having porosities. The rule of mixture is modified to describe and approximate material properties of the FG beams with porosity phases. Based on the present refined shear deformation beam theory, the equations of motion are derived from Hamilton's principle. The accuracy of the present solutions is verified by comparing the obtained results with the existing solutions. Illustrative examples are given also to show the effects of varying gradients, porosity volume fraction, aspect ratios, and thickness to length ratios on the free vibration of the FG beams.

2. Problem formulation

Consider a functionally graded beam with length L and rectangular cross section $b \times h$, with b being the width and h being the height as shown in Fig. 1. The beam is made of isotropic material with material properties varying smoothly in the thickness direction.

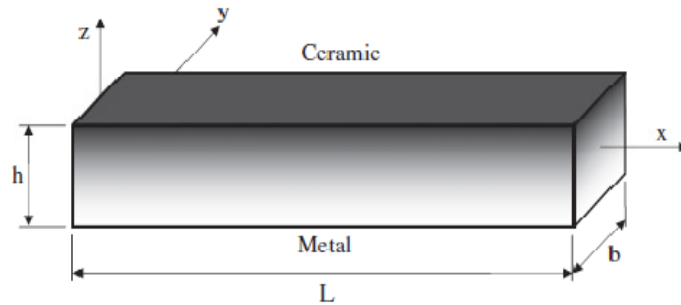


Fig. 1 Geometry and coordinate of a FG beam

2.1 Effective material properties of metal ceramic functionally graded beams

The properties of FGM vary continuously due to the gradually changing volume fraction of the constituent materials (ceramic and metal), usually in the thickness direction only. The power-law function is commonly used to describe these variations of materials properties. The expression given below represents the profile for the volume fraction.

A FG beam made from a mixture of two material phases, for example, a metal and a ceramic. The material properties of FG beams are assumed to vary continuously through the thickness of the beam. In this investigation, the imperfect beam is assumed to have porosities spreading within the thickness due to defect during production. Consider an imperfect FGM with a porosity volume fraction, $\alpha (\alpha \ll 1)$, distributed evenly among the metal and ceramic, the modified rule of mixture proposed by Wattanasakulpong and Ungbhakorn (2014) is used as

$$P = P_m \left(V_m - \frac{\alpha}{2} \right) + P_c \left(V_c - \frac{\alpha}{2} \right) \tag{1}$$

Now, the total volume fraction of the metal and ceramic is: $V_m + V_c = 1$, and the power law of volume fraction of the ceramic is described as

$$V_c = \left(\frac{z}{h} + \frac{1}{2} \right)^k \tag{2}$$

Hence, all properties of the imperfect FGM can be written as

$$P = (P_c - P_m) \left(\frac{z}{h} + \frac{1}{2} \right)^k + P_m - (P_c + P_m) \frac{\alpha}{2} \tag{3}$$

It is noted that the positive real number $k (0 \leq k \leq \infty)$ is the power law or volume fraction index, and z is the distance from the mid-plane of the FG plate. The FG beam becomes a fully ceramic plate when k is set to zero and fully metal for large value of k .

Thus, the Young’s modulus (E) and material density (ρ) equations of the imperfect FGM beam can be expressed as

$$E(z) = (E_c - E_m) \left(\frac{z}{h} + \frac{1}{2} \right)^k + E_m - (E_c + E_m) \frac{\alpha}{2} \quad (4)$$

$$\rho(z) = (\rho_c - \rho_m) \left(\frac{z}{h} + \frac{1}{2} \right)^k + \rho_m - (\rho_c + \rho_m) \frac{\alpha}{2} \quad (5)$$

However, Poisson's ratio (ν) is assumed to be constant. The material properties of a perfect FG beam can be obtained when α is set to zero.

In addition, for another scenario of porosity distribution, it is possible to obtain imperfect FGM samples which have almost porosities spreading around the middle zone of the cross-section and the amount of porosity seems to be on the decrease to zero at the top and bottom of the cross-section. Based on the principle of the multi-step sequential infiltration technique that can be employed to fabricate FGM samples (Wattanasakulpong *et al.* 2012), the porosities mostly occur at the middle zone. At this zone, it is difficult to infiltrate the materials completely, while at the top and bottom zones, the process of material infiltration can be performed easier and leaves less porosity. Consider this scenario, the equations of Young's modulus (E) and material density (ρ) in Eqs. (5)-(6) are replaced by the following forms

$$E(z) = (E_c - E_m) \left(\frac{z}{h} + \frac{1}{2} \right)^k + E_m - (E_c + E_m) \frac{\alpha}{2} \left(1 - \frac{2|z|}{h} \right) \quad (6)$$

$$\rho(z) = (\rho_c - \rho_m) \left(\frac{z}{h} + \frac{1}{2} \right)^k + \rho_m - (\rho_c + \rho_m) \frac{\alpha}{2} \left(1 - \frac{2|z|}{h} \right) \quad (7)$$

2.2 Basic assumptions

The assumptions of the present theory are as follows:

- (1) The origin of the Cartesian coordinate system is taken at the median surface of the FG beam.
- (2) The displacements are small in comparison with the height of the beam and, therefore, strains involved are infinitesimal.
- (3) The transverse displacement w includes two components of bending w_b , and shear w_s . These components are functions of coordinates x, y only.

$$w(x, z, t) = w_b(x, t) + w_s(x, t) \quad (8)$$

- (4) The transverse normal stress σ_z is negligible in comparison with in-plane stresses σ_x .
- (5) The axial displacement u in x -direction, consists of extension, bending, and shear components.

$$u = u_0 + u_b + u_s \quad (9)$$

The bending component u_b is assumed to be similar to the displacements given by the classical beam theory. Therefore, the expression for u_b can be given as

$$u_b = -z \frac{\partial w_b}{\partial x} \tag{10}$$

The shear component u_s gives rise, in conjunction with w_s , to the parabolic variation of shear strain γ_{xz} and hence to shear stress τ_{xz} through the thickness of the beam in such a way that shear stress τ_{xz} is zero at the top and bottom faces of the beam. Consequently, the expression for u_s can be given as

$$u_s = -f(z) \frac{\partial w_s}{\partial x} \tag{11}$$

$$f(z) = z - ze^{-2(z/h)^2} \tag{12}$$

2.3 Kinematics and constitutive equations

Based on the assumptions made in the preceding section, the displacement field can be obtained using Eqs. (2)-(6) as

$$u(x, z, t) = u_0(x, t) - z \frac{\partial w_b}{\partial x} - f(z) \frac{\partial w_s}{\partial x} \tag{13a}$$

$$w(x, z, t) = w_b(x, t) + w_s(x, t) \tag{13b}$$

The strains associated with the displacements in Eq. (13) are

$$\varepsilon_x = \varepsilon_x^0 + z k_x^b + f(z) k_x^s \tag{14a}$$

$$\gamma_{xz} = g(z) \gamma_{xz}^s \tag{14b}$$

where

$$\varepsilon_x^0 = \frac{\partial u_0}{\partial x}, \quad k_x^b = -\frac{\partial^2 w_b}{\partial x^2}, \quad k_x^s = -\frac{\partial^2 w_s}{\partial x^2}, \quad \gamma_{xz}^s = \frac{\partial w_s}{\partial x} \tag{14c}$$

$$g(z) = 1 - f'(z) \quad \text{and} \quad f'(z) = \frac{df(z)}{dz} \tag{14d}$$

The state of stress in the beam is given by the generalized Hooke's law as follows

$$\sigma_x = Q_{11}(z) \varepsilon_x \quad \text{and} \quad \tau_{xz} = Q_{55}(z) \gamma_{xz} \tag{15a}$$

where

$$Q_{11}(z) = E(z) \quad \text{and} \quad Q_{55}(z) = \frac{E(z)}{2(1+\nu)} \tag{15b}$$

2.4 Governing equations and boundary conditions

Hamilton's principle is used herein to derive the equations of motion. The principle can be stated in analytical form as (Thai and Vo 2012)

$$\delta \int_{t_1}^{t_2} (U - T) dt = 0 \quad (16)$$

where t is the time; t_1 and t_2 are the initial and end time, respectively; δU is the virtual variation of the strain energy and δT is the virtual variation of the kinetic energy. The variation of the strain energy of the beam can be stated as

$$\begin{aligned} \delta U &= \int_0^L \int_{-\frac{h}{2}}^{\frac{h}{2}} (\sigma_x \delta \varepsilon_x + \tau_{xz} \delta \gamma_{xz}) dz dx \\ &= \int_0^L \left(N \frac{d\delta u_0}{dx} - M_b \frac{d^2 \delta w_b}{dx^2} - M_s \frac{d^2 \delta w_s}{dx^2} + Q \frac{d\delta w_s}{dx} \right) dx \end{aligned} \quad (17)$$

where N , M_b , M_s and Q are the stress resultants defined as

$$(N, M_b, M_s) = \int_{-\frac{h}{2}}^{\frac{h}{2}} (1, z, f) \sigma_x dz_{ns} \quad \text{and} \quad Q = \int_{-\frac{h}{2}}^{\frac{h}{2}} g \tau_{xz} dz \quad (18)$$

The variation of the kinetic energy can be expressed as

$$\begin{aligned} \delta T &= \int_0^L \int_{-\frac{h}{2}}^{\frac{h}{2}} \rho(z) [\dot{u} \delta \dot{u} + \dot{w} \delta \dot{w}] dz dx \\ &= \int_0^L \left\{ I_1 [\dot{u}_0 \delta \dot{u}_0 + (\dot{w}_b + \dot{w}_s)(\delta \dot{w}_b + \delta \dot{w}_s)] - I_2 \left(\dot{u}_0 \frac{d\delta \dot{w}_b}{dx} + \frac{d\dot{w}_b}{dx} \delta \dot{u}_0 \right) \right. \\ &\quad + I_4 \left(\frac{d\dot{w}_b}{dx} \frac{d\delta \dot{w}_b}{dx} \right) - I_3 \left(\dot{u}_0 \frac{d\delta \dot{w}_s}{dx} + \frac{d\dot{w}_s}{dx} \delta \dot{u}_0 \right) + I_6 \left(\frac{d\dot{w}_s}{dx} \frac{d\delta \dot{w}_s}{dx} \right) \\ &\quad \left. + I_5 \left(\frac{d\dot{w}_b}{dx} \frac{d\delta \dot{w}_s}{dx} + \frac{d\dot{w}_s}{dx} \frac{d\delta \dot{w}_b}{dx} \right) \right\} dx \end{aligned} \quad (19)$$

where dot-superscript convention indicates the differentiation with respect to the time variable t ; $\rho(z)$ is the mass density; and $(I_1, I_2, I_3, I_4, I_5, I_6)$ are the mass inertias defined as

$$(I_1, I_2, I_3, I_4, I_5, I_6) = \int_{-\frac{h}{2}}^{\frac{h}{2}} (1, z, f, z^2, zf, f^2) \rho(z) dz \quad (20)$$

Substituting the expressions for δU and δT from Eqs. (17) and (19) into Eq.(16) and integrating

by parts versus both space and time variables, and collecting the coefficients of δu_0 , δw_b , and δw_s , the following equations of motion of the functionally graded beam are obtained

$$\delta u_0 : \frac{dN}{dx} = I_1 \ddot{u}_0 - I_2 \frac{d\ddot{w}_b}{dx} - I_3 \frac{d\ddot{w}_s}{dx} \tag{21a}$$

$$\delta w_b : \frac{d^2 M_b}{dx^2} = I_1 (\ddot{w}_b + \ddot{w}_s) + I_2 \frac{d\ddot{u}_0}{dx} - I_4 \frac{d^2 \ddot{w}_b}{dx^2} - I_5 \frac{d^2 \ddot{w}_s}{dx^2} \tag{21b}$$

$$\delta w_s : \frac{d^2 M_s}{dx^2} + \frac{dQ}{dx} = I_1 (\ddot{w}_b + \ddot{w}_s) + I_3 \frac{d\ddot{u}_0}{dx} - I_5 \frac{d^2 \ddot{w}_b}{dx^2} - I_6 \frac{d^2 \ddot{w}_s}{dx^2} \tag{21c}$$

Eq. (21) can be expressed in terms of displacements (u_0 , w_b , w_s) by using Eqs. (13), (14), (18) and (20) as follows

$$A_{11} \frac{\partial^2 u_0}{\partial x^2} - B_{11} \frac{\partial^3 w_b}{\partial x^3} - B_{11}^s \frac{\partial^3 w_s}{\partial x^3} = I_1 \ddot{u}_0 - I_2 \frac{d\ddot{w}_b}{dx} - I_3 \frac{d\ddot{w}_s}{dx} \tag{22a}$$

$$B_{11} \frac{\partial^3 u_0}{\partial x^3} - D_{11} \frac{\partial^4 w_b}{\partial x^4} - D_{11}^s \frac{\partial^4 w_s}{\partial x^4} = I_1 (\ddot{w}_b + \ddot{w}_s) + I_2 \frac{d\ddot{u}_0}{dx} - I_4 \frac{d^2 \ddot{w}_b}{dx^2} - I_5 \frac{d^2 \ddot{w}_s}{dx^2} \tag{22b}$$

$$B_{11}^s \frac{\partial^3 u_0}{\partial x^3} - D_{11}^s \frac{\partial^4 w_b}{\partial x^4} - H_{11} \frac{\partial^4 w_s}{\partial x^4} + A_{55}^s \frac{\partial^2 w_s}{\partial x^2} = I_1 (\ddot{w}_b + \ddot{w}_s) + I_3 \frac{d\ddot{u}_0}{dx} - I_5 \frac{d^2 \ddot{w}_b}{dx^2} - I_6 \frac{d^2 \ddot{w}_s}{dx^2} \tag{22c}$$

where A_{11} , D_{11} , etc., are the beam stiffness, defined by

$$(A_{11}, B_{11}, D_{11}, B_{11}^s, D_{11}^s, H_{11}^s) = \int_{-\frac{h}{2}}^{\frac{h}{2}} Q_{11} (1, z, z^2, f(z), z f(z), f^2(z)) dz \tag{23a}$$

and

$$A_{55}^s = \int_{-\frac{h}{2}}^{\frac{h}{2}} Q_{55} [g(z)]^2 dz \tag{23b}$$

3. Analytical solution

3.1 Effect reinforcement

The equations of motion admit the Navier solutions for simply supported beams. The variables u_0 , w_b , w_s can be written by assuming the following variations

$$\begin{Bmatrix} u_0 \\ w_b \\ w_s \end{Bmatrix} = \sum_{m=1}^{\infty} \begin{Bmatrix} U_m \cos(\lambda x) e^{i\omega t} \\ W_{bm} \sin(\lambda x) e^{i\omega t} \\ W_{sm} \sin(\lambda x) e^{i\omega t} \end{Bmatrix} \quad (24)$$

where U_m , W_{bm} , and W_{sm} are arbitrary parameters to be determined, ω is the eigenfrequency associated with m th eigenmode, and $\lambda = m\pi / L$.

Substituting the expansions of u_0 , w_b , w_s from Eqs. (24) into the equations of motion Eq. (22), the analytical solutions can be obtained from the following equations

$$\left(\begin{bmatrix} a_{11} & a_{12} & a_{13} \\ a_{12} & a_{22} & a_{23} \\ a_{13} & a_{23} & a_{33} \end{bmatrix} - \omega^2 \begin{bmatrix} m_{11} & m_{12} & m_{13} \\ m_{12} & m_{22} & m_{23} \\ m_{13} & m_{23} & m_{33} \end{bmatrix} \right) \begin{Bmatrix} U_m \\ W_{bm} \\ W_{sm} \end{Bmatrix} = \begin{Bmatrix} 0 \\ 0 \\ 0 \end{Bmatrix} \quad (25)$$

where

$$\begin{aligned} a_{11} &= A_{11}\lambda^2, & a_{12} &= -B_{11}\lambda^3, & a_{13} &= -B_{11}^s\lambda^3, \\ a_{22} &= D_{11}\lambda^4, & a_{23} &= D_{11}^s\lambda^4, & a_{33} &= H_{11}^s\lambda^4 + A_{55}^s\lambda^2 \end{aligned} \quad (26a)$$

$$\begin{aligned} m_{11} &= I_1, & m_{12} &= -I_2\lambda, & m_{13} &= -I_3\lambda, & m_{22} &= I_1 + I_4\lambda^2 \\ m_{23} &= I_1 + I_5\lambda^2, & m_{33} &= I_1 + I_6\lambda^2 \end{aligned} \quad (26b)$$

4. Results and discussion

In numerical analysis, fundamental frequencies of simply supported perfect and imperfect FG beams are evaluated. The FG beam is taken to be made of aluminum and alumina with the following material properties:

Ceramic (P_C : Alumina, Al_2O_3): $E_c = 380$ GPa; $\nu = 0.3$; $\rho_c = 3800$ kg/m³.
Metal (P_M : Aluminium, Al): $E_m = 70$ GPa; $\nu = 0.3$; $\rho_m = 270$ kg/m³.

And their properties change through the thickness of the beam according to power-law. The bottom surfaces of the FG beams are aluminum rich, whereas the top surfaces of the FG beams are alumina rich.

For convenience, the following dimensionless form is used

$$\bar{\omega} = \frac{\omega L^2}{h} \sqrt{\frac{\rho_m}{E_m}}$$

To validate accuracy of the proposed theory, the comparisons between the present results and the available results obtained by Simsek *et al.* (2010a) and Sina *et al.* (2009) is shown in Table 1.

Indeed, in Table 1, the non-dimensional natural frequencies for the perfect FG beam with $k = 0.3$ for different length-to-height ratios. As can be seen the results of the present theory are in good agreement with the other shear deformation theories.

Table 1 Comparison of non-dimensional fundamental frequencies of FG beams with $k = 0.3$.

$$\left(\bar{\omega} = \left(\omega L^2 / h \right) \sqrt{I_0 / \int_{-h/2}^{h/2} E(z) dz} \right)$$

Source	$L / h = 10$	$L / h = 30$	$L / h = 100$
FSDBT ^{R(*)}	2.701	2.738	2.742
FSDBT ^{S(*)}	2.701	2.738	2.742
PSDBT ^{R(*)}	2.702	2.738	2.742
PSDBT ^{S(*)}	2.702	2.738	2.742
ASDBT ^{R(*)}	2.702	2.738	2.742
ASDBT ^{S(*)}	2.702	2.738	2.742
Sina <i>et al.</i> (2009)	2.695	2.737	2.742
Present	2.702	2.738	2.742

(*) Results from Ref. (Simsek 2010a)

Table 2 Five Non-dimensional frequencies of FGM beam ($L/h = 5$)

k	α	$\bar{\omega}_1$	$\bar{\omega}_2$	$\bar{\omega}_3$	$\bar{\omega}_4$	$\bar{\omega}_5$
0.5	0	4.4118	15.4728	29.8929	45.8279	62.4877
	0.1	4.4053	15.4707	29.9251	45.9205	62.6586
	0.2	4.3939	15.4569	29.9444	46.0053	62.8317
1	0	3.9914	14.0224	27.1480	41.7120	56.9997
	0.1	3.9079	13.7669	26.7225	41.1454	56.3218
	0.2	3.7873	13.3939	26.0931	40.2962	55.2921
5	0	3.3991	11.5281	21.6924	32.6795	44.0756
	0.1	3.1448	10.6624	20.0789	30.2938	40.9317
	0.2	2.6924	9.1773	17.3940	26.4164	35.9187
10	0	3.2814	11.0264	20.5815	30.8108	41.3529
	0.1	3.0278	10.0958	18.7457	27.9794	37.4967
	0.2	2.5677	8.4726	15.6400	23.2907	31.2070

The first five dimensionless frequencies of perfect and imperfect FG beams are provided in Table 2. It should be noted that the materials properties are predicted using Eqs. (3)-(4). The results reveal that the frequency results decrease as the volume fraction of porosity (α) increases.

In Figs. 2 and 3, the effect of the porosity the fundamental frequencies of FG beams with two different types of porosity distribution is illustrated. It is noted that Solution I refers to the result of imperfect FG beams with evenly distributed porosities using Eqs. (3)-(4), while, Solution II is for the beams with another type of porosity distribution using Eqs. (6)-(7). It can be seen from Fig. 2 that the porosity leads to an increase of frequency and hence this type of porosity distribution (Solution I) makes the beam stiffer. However, the effect of porosity on fundamental frequencies

(Fig. 3) using Solution II is reversed and this type of porosity distribution makes the beam flexible.

In Fig. 4, the fundamental frequencies of imperfect FG beams with two different types of porosity distribution are plotted versus the power-law exponent (k). As observed, Solution II provides higher frequencies than those of Solution I; moreover, the frequencies increase with the increase of the power-law exponent (k) when this latter takes values more than 2.

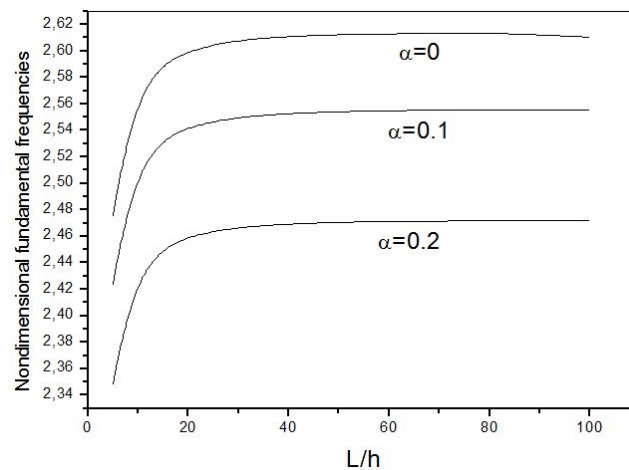


Fig. 2 Variation of the fundamental frequency $\left(\bar{\omega} = (\omega L^2 / h) \sqrt{I_0 / \int_{-h/2}^{h/2} E(z) dz} \right)$ of FG beams ($k = 1$) with L / h ratio for various values of the porosity volume fraction by considering the first solution

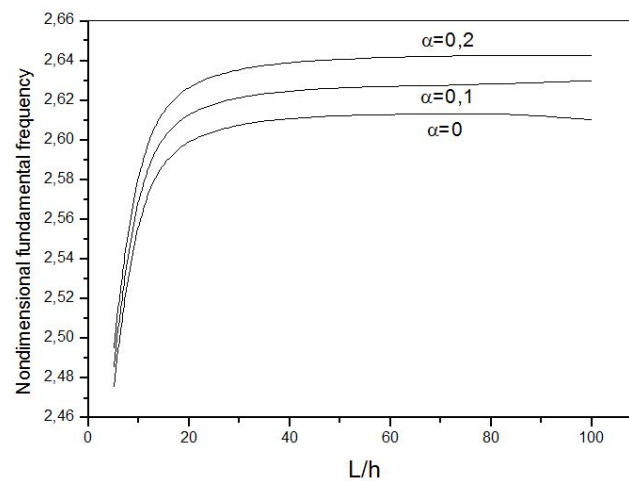


Fig. 3 Variation of the fundamental frequency $\left(\bar{\omega} = (\omega L^2 / h) \sqrt{I_0 / \int_{-h/2}^{h/2} E(z) dz} \right)$ of imperfect FG beams with power-law exponent k . ($L / h = 5, \alpha = 0.1$)

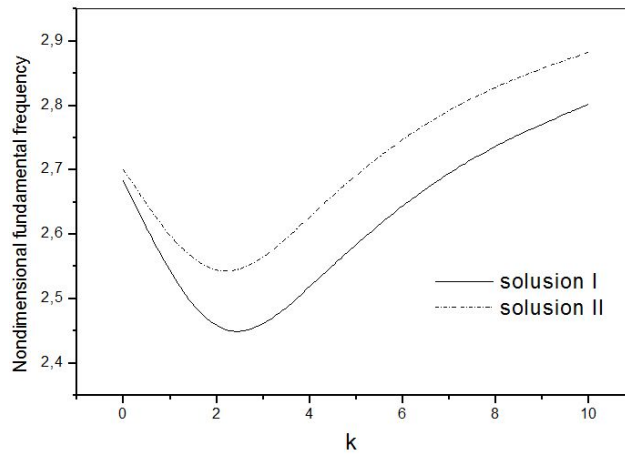


Fig. 4 Variation of the fundamental frequency $\left(\bar{\omega} = \left(\omega L^2 / h \right) \sqrt{I_0 / \int_{-h/2}^{h/2} E(z) dz} \right)$ of imperfect FG beams with power-law exponent k . ($L / h = 5$, $\alpha = 0.1$)

5. Conclusions

The exponential shear deformation beam theory is proposed for free vibration of perfect and imperfect FG beams. The theory accounts for parabolic distribution of the transverse shear strains and satisfies the zero traction boundary conditions on the surfaces of the beam without using shear correction factors. The modified rule of mixture covering porosity phases is used to describe and approximate material properties of the imperfect FG beams. It is based on the assumption that the transverse displacements consist of bending and shear components. Based on the present beam theory, the equations of motion are derived from Hamilton’s principle. The influence of the porosities on natural frequencies is then discussed. Numerical examples show that the proposed theory gives solutions which are almost identical with those obtained using other shear deformation theories.

Acknowledgments

The authors thank the referees for their valuable comments.

References

Ait Yahia, S., Ait Atmane, H., Houari, M.S.A. and Tounsi, A. (2015), “Wave propagation in functionally graded plates with properties using various”, *Struct. Eng. Mech., Int. J.*, **53**(6), 1143-1165.

Benatta, M.A., Tounsi, A., Mechab, I. and Bachir Bouiadjra, M. (2009), “Mathematical solution for bending of short hybrid composite beams with variable fibers spacing”, *Appl. Math. Comput.*, **212**(2), 337-348.

Bourada, M., Tounsi, A., Houari, M.S.A. and Adda Bedia, E.A. (2012), “A new four variable refined plate theory for thermal buckling analysis of functionally graded sandwich plates”, *J. Sandw. Struct. Mater.*, **14**(1), 5-33.

- Giunta, G., Crisafulli, D., Belouettar, S. and Carrera, E. (2011), "Hierarchical theories for the free vibration analysis of functionally graded beams", *Compos. Struct.*, **94**(1), 68-74.
- Hadji, L., Daouadji, T.H., Tounsi, A. and Adda Bedia, E.A. (2014), "A higher order shear deformation theory for static and free vibration of FGM beam", *Steel Compos. Struct., Int. J.*, **16**(5), 507-519.
- Kadoli, R., Akhtar, K. and Ganesan, N. (2008), "Static analysis of functionally graded beams using higher order shear deformation theory", *Appl. Math. Model.*, **32**(12), 2509-2525.
- Klouche Djedid, I., Benachour, A., Houari, M.S.A., Tounsi, A. and Ameer, M. (2014), "A n -order four variable refined theory for bending and free vibration of functionally graded plates", *Steel Compos. Struct., Int. J.*, **17**(1), 21-46.
- Li, X.-F. (2008), "A unified approach for analyzing static and dynamic behaviors of functionally graded Timoshenko and Euler-Bernoulli beams", *J. Sound Vib.*, **318**(4-5), 1210-1229.
- Merazi, M., Hadji, L., Hassaine Daouadji, T., Tounsi, A. and Adda Bedia, E. (2015), "A new hyperbolic shear deformation plate theory for static analysis of FGM plate based on neutral surface position", *Geomech. Eng., Int. J.*, **8**(3), 305-321.
- Nedri, K., El Meiche, N. and Tounsi, A. (2014), "Free vibration analysis of laminated composite plates resting on elastic foundations by using a refined hyperbolic shear deformation theory", *Mech. Compos. Mater.*, **49**(6), 641-650.
- Sallai, B.O., Tounsi, A., Mechab, I., Bachir, B.M., Meradjah, M. and Adda Bedia, E.A. (2009), "A theoretical analysis of flexional bending of Al/Al₂O₃ S-FGM thick beams", *Computat. Mater. Sci.*, **44**(4), 1344-1350.
- Simsek, M. (2010a), "Fundamental frequency analysis of functionally graded beams by using different higher-order beam theories", *Nucl. Eng. Des.*, **240**(4), 697-705.
- Simsek, M. (2010b), "Vibration analysis of a functionally graded beam under a moving mass by using different beam theories", *Compos. Struct.*, **92**(4), 904-917.
- Sina, S.A., Navazi, H.M. and Haddadpour, H. (2009), "An analytical method for free vibration analysis of functionally graded beams", *Mater. Des.*, **30**(3), 741-747.
- Tai, H.T. and Vo, P.V. (2012), "Bending and free vibration of functionally graded beams using various higher-order shear deformation beam theories", *Int. J. Mech. Sci.*, **62**(1), 57-66.
- Wattanasakulpong, N. and Ungbhakorn, V. (2014), "Linear and nonlinear vibration analysis of elastically restrained ends FGM beams with porosities", *Aerosp. Sci. Technol.*, **32**(1), 111-112.
- Wattanasakulpong, N., Prusty, B.G., Kelly, D.W. and Hoffman, M. (2012), "Free vibration analysis of layered functionally graded beams with experimental validation", *Mater. Des.*, **36**, 182-190.
- Zhong, Z. and Yu, T. (2007), "Analytical solution of a cantilever functionally graded beam", *Compos. Sci. Technol.*, **67**(3-4), 481-488.
- Zhu, J., Lai, Z., Yin, Z., Jeon, J. and Lee, S. (2001), "Fabrication of ZrO₂-NiCr functionally graded material by powder metallurgy", *Mater. Chem. Phys.*, **68**(1-3), 130-135.